Mutation Research 788 (2016) 32–40

Contents lists available at ScienceDirect

Mutation Research/Fundamental and Molecular Mechanisms of Mutagenesis

journal homepage: www.elsevier.com/locate/molmut
Community address: www.elsevier.com/locate/mutres

Charged particle mutagenesis at low dose and fluence in mouse splenic T cells

Dmytro Grygoryev[a], Stacey Gauny[b], Michael Lasarev[a], Anna Ohlrich[a], Amy Kronenberg[b], Mitchell S. Turker[a,c,*]

[a] Oregon Institute of Occupational Health Sciences, Oregon Health & Science University, Portland, OR 97239, United States
[b] Biological Systems and Engineering Division, Lawrence Berkeley National Laboratory, Berkeley, CA 94720, United States
[c] Molecular and Medical Genetics, Oregon Health & Science University, Portland, OR 97239, United States

ARTICLE INFO

Article history:
Received 18 February 2016
Received in revised form 25 March 2016
Accepted 28 March 2016
Available online 29 March 2016

Keywords:
Splenic T cells
Charged particle mutagenesis
Aprt mutation
Radiation signature mutations

ABSTRACT

High-energy heavy charged particles (HZE ions) found in the deep space environment can significantly affect human health by inducing mutations and related cancers. To better understand the relation between HZE ion exposure and somatic mutation, we examined cell survival fraction, *Aprt* mutant frequencies, and the types of mutations detected for mouse splenic T cells exposed *in vivo* to graded doses of densely ionizing ^{48}Ti ions (1 GeV/amu, LET = 107 keV/μm), ^{56}Fe ions (1 GeV/amu, LET = 151 keV/μm) ions, or sparsely ionizing protons (1 GeV, LET = 0.24 keV/μm). The lowest doses for ^{48}Ti and ^{56}Fe ions were equivalent to a fluence of approximately 1 or 2 particle traversals per nucleus. In most cases, *Aprt* mutant frequencies in the irradiated mice were not significantly increased relative to the controls for any of the particles or doses tested at the pre-determined harvest time (3–5 months after irradiation). Despite the lack of increased *Aprt* mutant frequencies in the irradiated splenocytes, a molecular analysis centered on chromosome 8 revealed the induction of radiation signature mutations (large interstitial deletions and complex mutational patterns), with the highest levels of induction at 2 particles nucleus for the ^{48}Ti and ^{56}Fe ions. In total, the results show that densely ionizing HZE ions can induce characteristic mutations in splenic T cells at low fluence, and that at least a subset of radiation-induced mutant cells are stably retained despite the apparent lack of increased mutant frequencies at the time of harvest.

1. Introduction

The health risks to astronauts from space radiation can arise at early times after exposure, such as radiation sickness and alterations in cognitive function, and as delayed effects including cancer, cardiovascular disease, neurodegenerative disease, and cataracts [1]. Accurate assessments of both early and delayed space radiation effects are required to make informed decisions about the best approach for long-term missions on the Moon or travel to and from Mars [2–5]. The most common charged particles in the space environment are protons present in the trapped radiation belts, in solar particle events (SPE), and among the galactic cosmic rays (GCR) [2]. Charged particles with high linear energy transfer (LET) that are also present in the GCR are of greater concern for the induction of mutations in somatic cells, due to their ability to deposit more energy locally. For example, we recently showed mutation induction by ^{48}Ti ions in mouse kidney epithelium at a fluence of one or two particles per cell nucleus [6]. Mutation induction is of significant concern because of the well-described relation between mutation and cancer [7].

Mouse *in vivo* mutation detection systems are used to study ionizing radiation mutagenesis because of the clear relation between mutation formation and cancer development [8]. *In vivo* systems allow radiation-induced mutations to form in the normal tissue environment, in which most cells are quiescent when irradiated. In the case of whole body exposure, the possible influences of systemic factors on mutation formation and on the persistence of mutant phenotypes *in vivo* are also included. *In vivo* mutation test systems include integrated bacterial transgenes [9–11], the X-linked selectable *Hprt* locus [12], and the autosomal *Aprt* [6,13], *Tk* [14], and *Dlb-1* [15,16] loci. Any cell type can be examined with integrated transgenes because mutation detection can be performed on DNA isolated directly from the exposed tissues; however these systems detect a limited spectrum of mutations (point mutations and

* Corresponding author at: Oregon Institute of Occupational Health Sciences, Oregon Health & Science University, 3181 SW Sam Jackson Park Road, Portland, OR 97239, United States.
E-mail address: turkerm@ohsu.edu (M.S. Turker).

http://dx.doi.org/10.1016/j.mrfmmm.2016.03.004
0027-5107/

small deletions). Selectable marker-based assays require cells that can divide outside the body to allow for selection and expansion of mutant cells prior to analysis, but these systems provide a more complete picture of the spectrum of radiation-induced mutations, particularly when autosomal loci are the targets [17]. Cell types used for these assays include splenic T cells, kidney epithelium, and ear fibroblasts [13,18].

Most *in vivo* radiation mutagenesis studies with selectable markers have examined the effects of X-rays and gamma-rays. For example, we showed that a relatively high dose of gamma rays (7.5 Gy) induced radiation signature mutations (large interstitial deletions and discontinuous loss of heterozygosity [LOH] patterns) inclusive of the selectable *Aprt* locus in the mouse kidney and ear [18]. Liang et al. showed that dose fractionation increased *Aprt* mutagenesis in mouse splenic T cells exposed to 4 Gy of X rays [13]. With regard to charged particle mutagenesis, we showed that the mouse kidney is a sensitive cell type for the detection of induced mutants with radiation signature mutations, including at low fluence for high LET ions [6,19,20]. The kidney epithelium is a biologically relevant cell target because epithelial cells give rise to radiogenic solid tumors [21].

Splenic T cells represent another biologically relevant cell type because ionizing radiation exposure also causes hematological cancers [21,22]. Several studies examining charged particle mutagenesis in the spleen have been reported, all of which used mice with integrated transgenes to screen for mutations [9,11,23,24]. To date, however, no charged particle mutagenesis experiments have performed with splenic T cells using an autosomal target to determine if radiation signature mutation can be detected. Here we report the mutagenic effects of high LET ^{48}Ti and ^{56}Fe ions in mouse splenic T cells at low dose and fluence, and for graded doses of protons.

2. Materials and methods

2.1. Mouse strain and irradiations

The experimental mice were *Aprt* heterozygous (*Aprt*$^{+/-}$) B6D2F1 hybrids from C57BL/6 X DBA/2 crosses. The C57BL/6 parent carried the *Aprt* knockout allele and the DBA/2 parent carried the wild type *Aprt* allele (Fig. 1A). Males and females in approximately equal numbers at six to seven months of age were transported from OHSU in Portland and were exposed to ^{48}Ti ions (1 GeV/amu, LET = 107 keV/μm, 0.2–1.4 Gy), ^{56}Fe ions (1 GeV/amu, LET = 151 keV/μm, 0.25–2.0 Gy), or protons (1 GeV, LET = 0.24 keV/μm, 0.5–5.0 Gy) at the NASA Space Radiation Laboratory (NSRL) at Brookhaven National Laboratory (BNL). The dose rates were 0.5–1 Gy/min depending upon total dose delivered. Sham-irradiated control mice traveled with each cohort of animals sent to BNL. These mice were also transported to the accelerator and handled in the same way as the irradiated mice. All experimental mice were returned to OHSU within two weeks after the irradiation, where the remainder of the work was performed.

The age range of the mice in these studies was chosen to approximate a biological age similar to that of a mid-career astronaut. Whole body exposures were conducted without anesthesia in small Plexiglas boxes with ventilation holes. Mice were positioned with their sides perpendicular to the beam path to minimize changes in energy deposited through the animal. In all runs, unexposed mice were used as sham controls. The numbers of mice used per dose and experiment are shown in Table 1. All animal work was conducted under protocols approved by OHSU and BNL. The estimated charged particle fluence for a given ion species and dose was calculated according to standard methods using the formula: fluence (per μm^2) = 6.24 D/L, where D is the dose in Gy, and L is the LET in keV/μm [25,26].

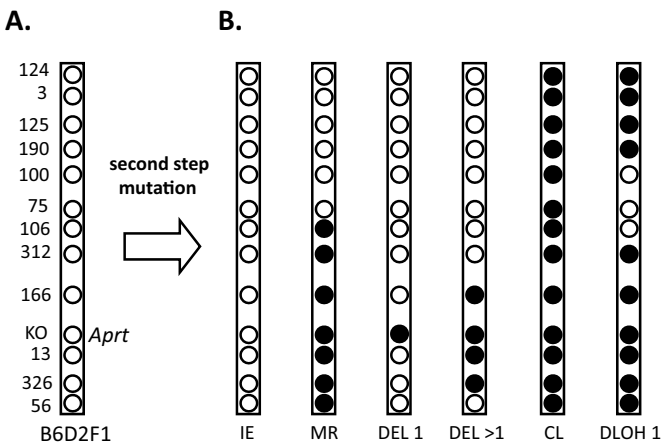

Fig. 1. Loss of heterozygosity (LOH) patterns reveal different mutational events. (A) The relative locations of polymorphic loci on mouse chromosome 8 that differ between the C57BL/6 and DBA2 mouse strains that were used to deduce the specific mutation present in each *Aprt* mutant examined in this study. The B6 (C57BL/6) derived chromosome contains a knockout (KO) *Aprt* allele that is non-functional. The D2 (DBA/2) derived chromosome contains an expressed, wild type *Aprt* allele, which is the target of mutation selection (*i.e.* loss of expression of this *Aprt* allele due to a mutational event allows a cell to grow in the presence of DAP in the culture medium). The numbers on the left side identify the chromosome 8 microsatellite loci that were examined in this study. These numbers omit the D8Mit prefix. (B) The PCR-based molecular analysis for loss (closed circles) or retention (open circles) of heterozygosity for polymorphic microsatellite sequences on mouse chromosome 8 in the *Aprt* mutant cells yields LOH patterns that can be used to classify each mutational event into one of 6 different categories. These are intragenic events (IE), apparent mitotic recombination (MR), interstitial deletion of *Aprt* polymorphic locus only (DEL 1), multilocus deletion (DEL > 1), chromosome loss (CL), and discontinuous LOH (DLOH). See text for more details.

Table 1
Exposure "runs" at Brookhaven National Laboratory by particle, dose and number of mice tested[a].

Run[b]	Sham[c]		protons[d]		^{56}Fe ions[d]		^{48}Ti ions[d]	
	Dose, Gy	Mice	Dose, Gy	Mice	Dose, Gy	Mice	Dose, Gy	Mice
1	0	8	5.0	10				
2	0	14	4.0	18	2.0	18	1.4	17
3	0	16			0.5	27	0.4	26
4	0	15	1.0	16	0.25	15		
5	0	13	0.5	20			0.2	20
							1.4	23
6	0	20	4.0	20	0.25	18		
					2.0	18		

[a] The number of mice tested for each condition is provided after the dose for that particle. For example, 10 mice were tested for the dose of 5.0 Gy protons.
[b] Each run represents a sham (control) set of mice and one or more charged particle exposures at Brookhaven National Laboratory (BNL). See Section 2 for more details.
[c] Sham mice were treated identically to exposed mice, including shipment to BNL and back to OHSU, with the exception of not being exposed to a charged particle. See Section 2 for more details.
[d] Mice were exposed to listed doses of protons, ^{56}Fe ions, and ^{48}Ti ions.

2.2. Cell culture and selection of Aprt mutants

Primary splenic T cells were isolated and stimulated as described [27], with modification [28]. The T cell preparations were set up from 3 to 5 months after irradiation because we were also isolating kidney epithelial *Aprt* mutants from the same mice [6] and prior worked showed that 3 months was required for maximal *Aprt* mutant frequency detection in this tissue [18]. RPMI 1640 medium (Fisher Scientific, New York, NY) was supplemented with 10 units

Table 2
Cloning efficiencies (CE) for splenic T cells.

(A) Cloning efficiencies from non-irradiated mice

Run[a]	CE[b]	95% CI[c]
1	0.105	0.066–0.168
2	0.067	0.050–0.090
3	0.033	0.026–0.044
4	0.052	0.039–0.071
5	0.052	0.039–0.070
6	0.080	0.068–0.080
Average	0.061	0.054–0.069

(B) Relative cloning efficiencies from irradiated mice

Particle	Run[d]	Dose, Gy	Relative CE[e]	95% CI[c]	P value[f]
Protons					
	5	0.5	0.94	0.66–1.33	0.732
	4	1	0.74	0.50–1.09	0.126
	2, 6	4	0.60	0.46–0.79	**<0.001**
	1	5	0.45	0.23–0.89	**0.023**
Fe ions					
	4, 6	0.25	0.74	0.54–0.94	**0.012**
	3	0.5	1.14	0.82–1.59	0.436
	2, 6	2	0.74	0.57–0.96	**0.021**
Ti ions					
	5	0.2	0.86	0.60–1.25	0.430
	3	0.4	0.93	0.67–1.28	0.641
	2, 5	1.4	0.76	0.59–0.99	**0.042**

[a] Each run represents a sham (control) set of mice and one or more charged particle exposures at Brookhaven National Laboratory (BNL).
[b] To determine cloning efficiencies, the number of clones observed under non-selective conditions was divided by the total number of cells plated. See Section 2 for more details.
[c] 95% confidence interval for relative cloning efficiency (CE).
[d] Mice were exposed to listed doses protons, ^{56}Fe ions, and ^{48}Ti ions. "Run" refers to specific experiment, as shown in Table 1.
[e] For the determination of relative cloning efficiencies (CE) after charged particle exposures, the cloning efficiency for a given exposure was divided by the cloning efficiency measurement obtained from non-irradiated mice used in the same run.
[f] P values <0.05 were considered statistically significant. The significant values are highlighted in bold.

of mouse recombinant IL-2/ml medium, 10% rat T-STIM supplement with Con A (10 μg/ml) (Becton Dickinson Labware, Bedford, MA) and 10% fetal bovine serum. Extra Con A was added at 4 μg/ml medium for overnight mitogenic stimulation. After overnight stimulation, cells were counted, diluted to 4×10^5 cells/ml and seeded for *Aprt* mutant selection into three or four 96-well U-bottom microtiter dishes (100 μl per well) supplemented with 50 μg/ml of 2,6-diaminopurine (DAP) (Sigma, St Louis, MO).

Cloning efficiencies (CE) were determined as described [27]. A sample of each primary culture was diluted with complete medium to 50 cells/ml and plated in aliquots of 100 μl per well in one 96-well microtiter dish in the presence of 4×10^4 lethally irradiated (100 Gy) mouse T cells per well. Plates were scored for colony growth on day 10. The number of colony-forming units per well on the CE and DAP plates was calculated as described [29].

Aprt mutant colonies from sham-irradiated and charged particle-exposed mice were expanded as described by others [27], with some modification. The mutant clones were transferred into 24-well microtiter plates with each well containing one ml of RPMI medium with Con A (4 μg/ml), DAP and FBS. The clones were refed with 1 ml mitogen-free medium including DAP after 3 days. After an additional 7 days of growth, DNA was isolated from clones as described in the next section.

2.3. Molecular analysis

Genomic DNA from expanded *Aprt* mutant clones was isolated as described in Ref. [27]. To release DNA, cells were pipetted into Eppendorf tubes and washed with PBS; cell pellets were resuspended in 20 μl of digestion mix comprised of Tween 20 0.5% (vol/vol) and 0.1 mg of proteinase K per ml in lx PCR buffer, incubated at 55 °C for 6 h, and then incubated at 95 °C for 10 min.

In general, no more than 4 mutants were examined from a given spleen. To determine the mechanisms underlying *Aprt* mutation, each DNA preparation was examined by PCR amplification for retention or loss of heterozygosity of 13 polymorphic microsatellite loci on chromosome 8 (Invitrogen, Carlsbad, CA) (Fig. 1), including a microsatellite sequence located immediately upstream of *Aprt* [30]. The LOH analyses were conducted at the Plant-Microbe Genomics Facility at Ohio State University, which uses an ABI Prism 3700 DNA analyser to separate fluorescently labelled PCR products.

2.4. Statistical analysis

Cloning efficiencies (CE) and mutant frequencies (MF) were calculated according to standard methods [31]. Each response was log-transformed and then analyzed using a general linear model. Robust standard errors were used for estimation and testing to allow for some heteroscedasticity. The mean response computed on the log scale estimates the median response on the original scale, and differences comparing a given radiation dose to control (on the log scale) represent multiplicative (*i.e.*, relative) changes for the median response on the original scale [32]. Models were separately fitted for each particle (protons, ^{48}Ti ions, ^{56}Fe ions).

Binomial logistic regression was used to explore the association between the proportion of each type of mutation and radiation dose. Tests were performed to determine whether there was an overall effect (odds differ among the three doses of radiation, treated as three distinct categories) and also whether the odds of a specific mutation followed a linear trend over radiation dose. Odds ratios (OR; comparing odds of a mutation for each dose relative to control) were computed together with 95% confidence intervals for each dose. In some instances the OR was not defined (due to

Table 3
Aprt Mutant frequencies for splenic T cells.

(A) Mutant frequencies for non-irradiated spleens

Run[a]	Mutant Frequency[b]	95% CI[c]
1	2.64	1.49–4.67
2	2.49	1.44–4.28
3	3.78	2.68–5.35
4	1.32	0.87–1.99
5	3.59	2.17–5.94
6	2.99	2.15–4.18
Average	2.66	2.21–3.20

(B) Mutant frequencies for irradiated spleens

Particle	Run[d]	Dose, Gy	Mutant Freq.[e]	95% CI[c]	P value[f]
Protons					
	5	0.5	0.85	0.43–1.56	0.596
	4	1	1.80	0.92–3.54	0.087
	2, 6	4	1.02	0.66–1.59	0.924
	1	5	4.57	2.16–9.64	**<0.001**
Fe ions					
	4, 6	0.25	1.13	0.76–1.67	0.544
	3	0.5	0.73	0.44–1.12	0.204
	2, 6	2	1.20	0.80–1.80	0.376
Ti ions					
	5	0.2	0.91	0.51–1.62	0.747
	3	0.4	0.90	0.54–1.50	0.694
	2, 5	1.4	0.86	0.54–1.36	0.517

[a] Each run represents a sham (control) set of mice and one or more charged particle exposures at Brookhaven National Laboratory (BNL).
[b] Mutant frequencies are $\times 10^{-6}$.
[c] 95% confidence interval $\times 10^{-6}$.
[d] Mice were exposed to listed doses of protons, ^{56}Fe ions, and ^{48}Ti ions. "Run" refers to specific experiment as shown in Table 1.
[e] For the determination of relative mutant frequency after charged particle exposures, the mutant frequency for a given exposure was divided by the mutant frequency obtained from non-irradiated mice used in the same run.
[f] P values <0.05 were considered statistically significant. The one significant value (5 Gy protons) is highlighted in bold.

zero observed mutations); in these cases Parzen's median unbiased estimate of the odds ratio (and 95% CI) was computed [33].

3. Results

3.1. Study sets

The charged particle exposures were conducted in 6 separate experimental "runs" at the Brookhaven National Laboratory (BNL) (Upton, New York). The specific exposures tested for each run and numbers of mice that were used for these exposures are shown in Table 1.

3.2. Toxicity from exposures

We used relative cloning efficiencies for the splenic T cells as a measure of toxicity from the exposures. These measures are for persistent toxic effects because the cloning efficiency assays were set up 3–5 months after the mice were exposed, at the same time the mutant frequency assays were set up (see below). We measured cloning efficiencies for splenic T cells from non-irradiated mice from 6 independent experiments and found an average cloning efficiency of 6.1% (CI, 5.4–6.9%) (Table 2A). For the determination of changes in cloning efficiencies after charged particle exposures, we used the specific cloning efficiency measurement from non-irradiated mice used in the same run.

Statistically significant decreases in cloning efficiencies were observed at the time of tissue harvest for all three particles at the highest doses tested (Table 2B). The largest decreases were for high dose proton exposures, with relative cloning efficiencies for 4 and 5 Gy exposures of 60% ($p < 0.001$) and 45% ($p = 0.023$), respectively. A decrease in the relative cloning efficiency to 74% was observed for 1 Gy proton exposure; however this decrease was not statistically significant ($p = 0.126$). The decreases in relatively cloning efficiencies for 2 Gy Fe ions and 1.4 Gy Ti ions were 74% and 76%, respectively, and these decreases were statistically significant ($p = 0.041$ and $p = 0.021$, respectively). The only other observed decrease that reached statistical significance was for the lowest dose of Fe ion tested (0.25 Gy), which was at a relative cloning efficiency level of 74% ($p = 0.012$). We note that this was the only low dose for which two independent cloning efficiency assays were performed, which doubled the number of mice used and increased statistical power.

3.3. Aprt *mutant frequency determinations*

Aprt mutant frequency assays were set up at the same time as the cloning efficiency determinations, 3–5 months following irradiation. Six independent groups of sham-irradiated mice were also used to determine the spontaneous mutant frequency for the cohorts shipped to and from Brookhaven. The spontaneous mutant frequencies ranged from 1.32 to 3.78×10^{-6}, with an average of 2.66×10^{-6} (95% CI, 2.21–3.20) (Table 3A).

A >4 fold increase in *Aprt* mutant frequency was observed for spleens exposed to 5 Gy of protons. Otherwise, no significant increase in *Aprt* mutant frequencies was observed for any condition tested (Table 3B).

3.4. Spontaneous mutation spectra

The expressed *Aprt* allele in the B6D2F1 heterozygous strain is derived from the DBA/2 parent. Thus, large mutational events leading to loss of *Aprt* expression result in LOH events for markers on the DBA/2-derived chromosome 8 homologue. We used a LOH

Table 4
Proton Mutation Spectra[a].

Dose, Gy[b]		IE	MR	CL	D = 1	D > 1	DLOH	Total[c]	RS
0	Number	56	52	16	9	3	5	141	8
	%	39.7	36.9	11.3	6.4	2.1	3.5	100	5.7
0.5	Number	24	11	10	0	1	8	54	9
	%	44.4	20.4	18.5	0	1.9	14.8	100	16.7
	p value[d]	0.548	**0.020**	0.192	**0.014***	0.826	**0.005**		**0.007**
1.0	Number	2	3	4	3	1	2	15	3
	%	13.3	20.0	26.7	20.0	6.7	13.3	100	20.0
	p value[d]	0.062	0.174	0.104	0.076	0.202	0.069		**0.025**
4.0	Number	9	27	5	5	3	0	49	3
	%	18.4	55.1	10.2	10.2	6.1	**0**	100	6.1
	p value[d]	**0.008**	**0.042**	0.826	0.382	0.104	0.120*		0.598
	p overall[e]	**0.006**	**0.002**	0.221	**0.026**	0.250	**0.001**		**0.011**
	p trend[e]	**0.004**	**0.013**	0.704	0.222	0.074	0.213		0.976

[a] Based on LOH pattern (see Fig. 1 and text), mutations were classified as 1) intragenic events (IE), 2) apparent mitotic recombination (MR), 3) chromosome loss (CL), 4) deletion of the Aprt locus only (D = 1), 5) multilocus deletion (D > 1), and 6) discontinuous LOH (DLOH). Radiation signature mutations were obtained by adding D > 1 and DLOH columns. For each mutation by dose category, the number and percentage of mutant cells exhibiting a particular mutation is given, as is the p value relative to the sham control.

[b] Doses were 0.5, 1.0, and 4.0 Gy protons (1 GeV) and sham (0).

[c] The total number of mutant cells examined for each dose.

[d] P values <0.05 were considered statistically significant. Significant values are highlighted in bold. Entries marked with an asterisk have an estimated odds ratio computed using Parzen's median unbiased estimator.

[e] P overall is the p value for all three doses combined relative to sham control. P trend looks for a trend in the change in percentage for a given mutation as a function of dose. Significant values are highlighted in bold.

analysis for 13 polymorphic loci on mouse chromosome 8 in the B6D2F1 background, including one located 1 kb upstream of the *Aprt* promoter, to identify the types of mutations leading to loss of *Aprt* expression (Fig. 1B). These are 1) intragenic events (point mutations and epigenetic silencing), 2) apparent mitotic recombination, 3) chromosome loss, 4) deletion of the *Aprt* locus only, as defined by LOH only for the *Aprt* microsatellite, 5) multilocus deletion including *Aprt* and at least one linked microsatellite repeat locus, and 6) discontinuous LOH, as defined by at least one LOH tract not apparently linked to the mutation causing loss of *Aprt* expression [34].

The spectrum of spontaneous mutation was determined from 141 mutant clones that were collected from experiments 2–6 (Table 1). As shown in Table 4 (and repeated in Tables 5 and 6), the predominant spontaneous mutation types were intragenic events (IE, 39.7%) and mitotic recombination (MR, 36.9%), with the two next most common being chromosome loss (CL, 11.3%) and deletion of the *Aprt* microsatellite marker only (D = 1, 6.4%). The two least common spontaneous mutational events were discontinuous LOH (3.5%) and multilocus interstitial deletion (2.1%).

3.5. Mutation spectra as a function of radiation type and dose

The spontaneous mutation spectrum was used as the baseline for comparisons with the mutation spectra for *Aprt* mutant T cells isolated from spleens exposed to protons (0.5, 1.0, and 4.0 Gy), ^{56}Fe ions (0.25, 0.5, and 2.0 Gy), and ^{48}Ti ions (0.2, 0.4, and 1.4 Gy). For this comparison we added an additional mutation category termed radiation signature (RS), which was made by pooling the large interstitial deletion (D > 1) and discontinuous LOH categories. This decision was based on the relatively low spontaneous percentage for each category and work with the kidney epithelium showing that these mutations are significantly induced by gamma radiation and charged particle exposures [6,18,19]. The number of mutants cells analyzed was considered sufficient for 8 of the 9 conditions (from 37 to 91 mutant cells analyzed, Tables 4–6). Only 15 mutant clones were collected for the 1.0 Gy proton exposure (Table 4), though this group was also included in the statistical analysis for the sake of completeness.

Tables 4–6 provide the mutation spectra data for T cell mutants isolated from spleens of mice irradiated with protons, ^{56}Fe ions, and ^{48}Ti ions, respectively. The types of mutations considered are shown in Fig. 1B. In each case the relative number of mutations for each category was compared against the same type of mutations within the spontaneous spectrum and p values determined to identify significant changes as a result of exposure. Because three doses were examined for each type of charged particle radiation, we also determined whether exposure itself was correlated with a significant change (p overall) and whether a trend as a function of dose could be discerned (p trend).

The most consistent observation made when considering all three charged particle exposures was the induction of radiation signature mutations, with significant overall increases for all 3 charged particles. P overall is 0.011 for protons, 0.008 for ^{56}Fe ions, and <0.001 for ^{48}Ti ions. However, closer inspection of the different doses tested revealed that these significant differences were essentially driven by doses in the range of 0.4 Gy (^{48}Ti ions, $p < 0.001$) to 0.5 Gy (protons, $p = 0.007$ and ^{56}Fe ions, $p = 0.002$) (Fig. 2). Within the radiation signature category at these doses, increases in discontinuous LOH events were significant for protons ($p = 0.005$) and ^{56}Fe ions ($p = 0.005$), but only marginal for ^{48}Ti ions ($p = 0.062$). The predominant change for ^{48}Ti ions at 0.4 Gy was an increase in large interstitial deletions from 2.1% for spontaneous mutants to 22.5% for exposed spleens. Another finding that was noted for both heavy ions was the induction of chromosome loss events at the lowest dose and fluence tested. The increase for 0.2 Gy ^{48}Ti ions, relative to spontaneous mutants was from 11.3% to 22.5% ($p = 0.030$). The increase for 0.25 Gy ^{56}Fe ions was from 11.3% to 31.0% ($p = 0.001$).

The relative percentage of *Aprt* mutant T cell clones exhibiting mitotic recombination LOH patterns was decreased relative to the spontaneous mutants (36.9%) for all three charged particle exposures at the lower doses, particularly in the range in which the radiation signature mutants were induced. These decreases were significant for 0.4 Gy ^{48}Ti ions (8.2%, $p = 0.002$ and 0.5 Gy) protons (20.4%, $p = 0.020$), but not for ^{56}Fe ions (29.3%, $p = 0.231$). A significant increase in apparent mitotic recombination events was only observed for 4 Gy protons (55.1%, $p = 0.042$).

Table 5
^{56}Fe ion mutation spectra[a].

Dose, Gy[b]		IE	MR	CL	D = 1	D > 1	DLOH	Total[c]	RS
0	Number	56	52	16	9	3	5	141	8
	%	39.7	36.9	11.3	6.4	2.1	3.5	100	5.7
0.25	Number	14	17	18	2	2	5	58	7
	%	24.1	29.3	31.0	3.4	3.4	8.6	100	12.1
	p value[d]	**0.039**	0.231	**0.001**	0.418	0.369	0.089		0.052
0.5	Number	18	8	2	1	2	6	37	8
	%	48.6	21.6	5.4	2.7	5.4	16.2	100	21.6
	p value[d]	0.328	0.062	0.297	0.402	0.175	**0.005**		**0.002**
2.0	Number	25	27	6	6	5	1	70	6
	%	35.7	38.6	8.6	8.6	7.1	1.4	100	8.6
	p value[d]	0.843	0.969	0.536	0.562	**0.049**	0.535		0.211
	p overall[e]	0.080	0.186	**<0.001**	0.517	0.185	**0.003**		**0.008**
	p trend[e]	0.837	0.727	0.194	0.390	**0.042**	0.368		0.530

[a] Based on LOH pattern (see Fig. 1 and text), mutations were classified as 1) intragenic events (IE), 2) apparent mitotic recombination (MR), 3) chromosome loss (CL), 4) deletion of the Aprt locus only (D = 1), 5) multilocus deletion (D > 1), and 6) discontinuous LOH (DLOH). Radiation signature mutations were obtained by adding D > 1 and DLOH columns. For each mutation by dose category, the number and percentage of mutant cells exhibiting a particular mutation is given, as is the p value relative to the sham control.
[b] Doses were 0.25, 0.5 and 2.0 Gy ^{56}Fe ions (1 GeV/amu) and sham (0).
[c] The total number of mutant cells examined for each dose.
[d] P values <0.05 were considered statistically significant. Significant values are highlighted in bold.
[e] P overall is the p value for all three doses combined relative to sham control. P trend looks for a trend in the change in percentage for a given mutation as a function of dose. Significant values are highlighted in bold.

Table 6
^{48}Ti ion mutation spectra[a].

Dose, Gy[b]		IE	MR	CL	D = 1	D > 1	DLOH	Total[c]	RS
0	Number	56	52	16	9	3	5	141	8
	%	39.7	36.9	11.3	6.4	2.1	3.5	100	5.7
0.2	Number	35	21	18	3	0	3	80	3
	%	43.8	26.2	22.5	3.8		3.8	100	3.8
	p value[d]	0.558	0.071	**0.030**	0.412	0.179*	0.710		0.855
0.4	Number	26	4	0	4	11	4	49	15
	%	53.1	8.2		8.2	22.5	8.2	100	30.6
	p value[d]	**0.004**	**0.002**	**0.004***	0.412	**<0.001**	0.062		**<0.001**
1.4	Number	38	25	13	5	1	4	86	5
	%	44.2	29.1	15.1	5.8	1.2	4.7	100	5.8
	p value[d]	0.757	0.091	0.510	0.782	0.834	0.528		0.665
	p overall[e]	**0.025**	**0.005**	**0.006**	0.561	**<0.001**	0.243		**<0.001**
	p trend[e]	0.942	0.199	0.889	0.902	0.797	0.644		0.876

[a] Based on LOH pattern (see Fig. 1 and text), mutations were classified as 1) intragenic events (IE), 2) apparent mitotic recombination (MR), 3) chromosome loss (CL), 4) deletion of the Aprt locus only (D = 1), 5) multilocus deletion (D > 1), and 6) discontinuous LOH (DLOH). Radiation signature mutations were obtained by adding D > 1 and DLOH columns. For each mutation by dose category, the number and percentage of mutant cells exhibiting a particular mutation is given, as is the p value relative to the sham control.
[b] Doses were 0.2, 0.4, and 1.4 Gy ^{48}Ti ions (1 GeV/amu) and sham (0).
[c] The total number of mutant cells examined for each dose.
[d] P values <0.05 were considered statistically significant. Significant values are highlighted in bold. Entries marked with an asterisk have an estimated odds ratio computed using Parzen's median unbiased estimator.
[e] P overall is the p value for all three doses combined relative to sham control. P trend looks for a trend in the change in percentage for a given mutation as a function of dose. Significant values are highlighted in bold.

4. Discussion

We report here the mutagenic effect of charged particle exposure on the spectra of *Aprt* mutations in mouse splenic T cells. The predominant spontaneous mutations were intragenic events (*i.e.*, base pair changes and/or epigenetic silencing) [18,35] and apparent mitotic recombination, each at levels near 40%. Chromosome loss, which represents approximately half of all spontaneous *Aprt* mutations in the kidney epithelium [31], was found in only 11% of the spontaneous splenic T cell mutants. The least common spontaneous *Aprt* mutations in the splenic T cells were large interstitial deletions and discontinuous LOH patterns. Both are induced by charged particle exposure and gamma radiation in the kidney epithelium, and thus are considered "radiation signature" mutations [6,18,19,36].

The spontaneous *Aprt* mutation spectrum we observed in splenic T cells in the B6D2F1 hybrid is somewhat distinct from that reported by Liang et al. in C57BL/6 X C3H/He hybrids, where mitotic recombination was found in more than half of all mutant cells [13]. That group showed earlier that the frequency of mitotic recombination is dependent on the degree of sequence divergence [37], which could explain the differences in our respective observations with different hybrid strains. Nonetheless, spontaneous "radiation signature" mutations were also rare in their study, as we report here, and were induced by ionizing radiation (X-ray) exposure with either a single or fractionated exposures totaling 4 Gy. Spleens were harvested in their experiments at 2 months after the last exposure [13].

The major observation made in the current study is that high LET charged particles are mutagenic in mouse T cells at low fluence, as

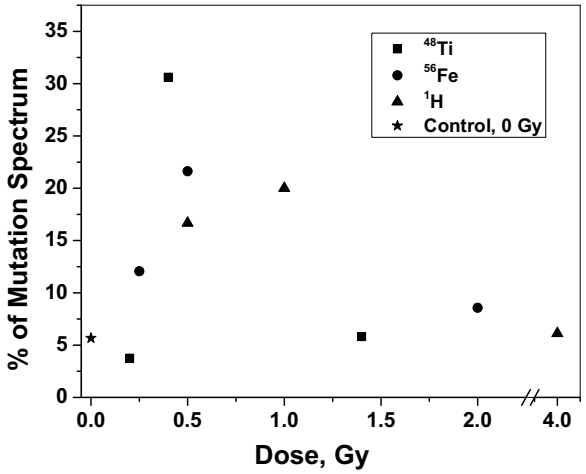

Fig. 2. Fraction of radiation signature mutations as a function of dose. The percentage of radiation signature mutations (D > 1 + DLOH, see Fig. 1B) is plotted by dose. The charged particles tested are protons (▲), ^{56}Fe ions (●), and ^{48}Ti ions (■). Spontaneous radiation signature percentage is included (★).

demonstrated by the changes in the mutation spectra when compared with spontaneously-arising mutants. A significant increase in chromosome loss was detected for both ^{48}Ti ions and ^{56}Fe ions at the lowest doses tested, 0.2 and 0.25 Gy, respectively, relative to the spontaneous spectrum. These doses represent an average fluence of approximately 1 traversal per nucleus for the T cells. In this situation, 37% of the cells are not traversed by a heavy ion track, 37% of the cells are traversed by a single heavy ion track, and the remainder of the cells are traversed by two or more heavy ion tracks. An increase in radiation signature mutations (large interstitial deletions and discontinuous LOH patterns) was also observed at 0.25 Gy ^{56}Fe ions, although this increase was just short of significance ($p = 0.052$). Radiation signature mutations were induced at an average of two particle traversals per cell nucleus for both ^{48}Ti ions and ^{56}Fe ions, though interstitial deletions were the predominant induced radiation signature mutation for 0.4 Gy ^{48}Ti ions, whereas discontinuous LOH events were more common for 0.5 Gy ^{56}Fe ions. Radiation quality might play a role in the types of mutation that are induced, though all radiation signature mutations are likely a result of two or more double strand breaks. We grouped both mutation patterns under the heading of radiation signature mutations because in our work with kidney epithelial cells we observed that both types were induced by high doses of protons and ^{56}Fe ions [19,36], and by the same doses of ^{48}Ti ions used in this study [6].

A general rule in radiation mutagenesis is that increased mutant frequencies correlate with exposure-induced mutations in a dose dependent manner [18,20,38–44]. This general rule holds quite well for work with cultured cells because the time between exposure and the process of setting up assays to select mutant cells is usually a week or less. In contrast, investigators using *in vivo* mutation systems often wait significantly longer than a week after radiation exposure to begin identifying and isolating mutant cells [13,18,44]. One reason for this longer wait time is that one or more cell divisions are required for an induced mutation to be established within a cell and, unlike cultured cells, most cells *in situ* are quiescent when exposed and can remain quiescent for indeterminate times after exposure. Specifically, for *in vivo* radiation mutagenesis in the kidney, we found that 2–3 months are necessary for maximal levels of *Aprt* mutant frequencies to be observed [18].

We have data for charged particle mutagenesis in the kidney epithelium of B6D2F1 mice that agree with the noted rule that mutant frequencies increase as a function of radiation dose [6,18,20,39], though the slopes of observed increases in mutant frequencies were particle specific. We observed a linear increase for kidney *Aprt* mutant frequencies as a function of dose for ^{56}Fe ions [39] that remained stable from 3 to 9 months after irradiation. We also observed a curvilinear increase for proton exposures that was particularly evident at higher doses (4 and 5 Gy) [20], and that also remained stable from 3 to 9 months after irradiation. For ^{48}Ti ion exposures in the kidney, we observed an increase from 0.2 to 0.4 Gy, but not from 0.4 to 1.4 Gy (though we did not measure doses between 0.4 and 1.4 Gy) [6]. Finally, we observed an increased mutant frequency for 7.5 Gy of ^{137}Cs gamma rays, the only dose tested in those experiments, that also remained stable from 3 to 9 months [18]. In all cases, we observed that radiation signature mutations were induced and retained after high dose exposures in the kidney [6,18,19,36].

In contrast to the kidney epithelium, we did not observe increased mutant frequencies for splenic T cells, except at the highest dose tested (5.0 Gy protons). Similarly, no increase in *Aprt* mutant frequencies was observed in B6C3F1 mice exposed to a single dose of 1, 2, or 4 Gy of X-rays [13]. Nonetheless, the mutation spectra work (Tables 4–6 and Fig. 2) clearly demonstrates that the charged particle exposures induced radiation signature mutations in the splenic T cells, particularly at relatively low doses and fluence, and induced whole chromosome loss at the lowest doses and fluences tested for ^{48}Ti ions and ^{56}Fe ions.

The question, therefore, is how to account for the induction of mutations by charged particles in the absence of increased mutant frequencies in our data. We speculate that the lack of an observed increase in mutant frequency is not due to the lack of induction of *Aprt* mutations, but instead reflects loss of mutant cells over time due to apoptosis, selective removal, and/or reduced growth rates. For example, in a study of proton-induced mutations in the mouse spleen using the bacterial *lacZ* reporter transgene, mutant frequencies were found to increase from 1 to 8 weeks, but then decreased from 8 to 16 weeks [45]. In another study using gamma radiation to induce *Hprt* mutant cells in the mouse spleen, the mutant frequencies were found highest at 3–5 weeks after irradiation, and then decreased at subsequent time points before rising again at 30–50 weeks after exposure [46]. Those studies suggest that radiation-induced mutant frequencies can change as a function of time in the mouse spleen, and the possibility exists that we missed a presumed increased that occur prior to the 3–5 month window we used to collect *Aprt* mutants. A second possibility is that the mouse T cells are more prone to apoptosis after exposure, which would be consistent with work by others showing increased *Aprt* mutant frequencies in X-irradiated mouse spleens when apoptosis rates were decreased by a weekly fractionation regimen for a given dose [13]. A third possibility is that charged particle-induced *Aprt* mutant cells have more extensive damage on average than non-mutant cells, and therefore would be at a growth disadvantage as the spleen repopulates after exposure and/or undergoes normal turnover. Thus, the apparent lack of an increase in *Aprt* mutant frequency in the spleen could reflect a balance between an initial increase in mutant frequency followed by an apparent decrease because less heavily damaged non-mutant cells would have a proliferative advantage. Still another possibility is that the most common charged particle-induced mutation, apparent mitotic recombination [6,19,36], is not significantly induced in the splenic T cells, though we did observe induction at high dose protons (see Table 4). Interestingly, most charged particle-induced mutants with the apparent mitotic recombination pattern in kidney epithelial cells are due to non-reciprocal translocations [6,36].

Clearly, further work is required to test these different possibilities. We also note the likelihood that the various hypotheses listed here are not mutually exclusive.

Most importantly, the majority of the radiation signature mutations we observed in this study, and likely a subset of other

mutations as well, were induced by charged particle exposure and T cells bearing these mutations persisted for many months after exposure. Thus, they represent induced mutant cells that are of most interest when considering the malignant process. In this regard we can compare our results with those for charged particle-induced hematological and other tumors for which dose response data are available at low doses. One comparison is with a study reported by Weil et al. that examined the induction of both acute myeloid leukemia (AML) and liver cancer in sensitive mice exposed to ^{28}Si and ^{56}Fe ions at doses that ranged from 0.1 to 1.0 Gy. For AML, they observed a peak of induction at 0.2 Gy for ^{56}Fe ions that declined at higher doses, and a plateau for ^{28}Si ions at doses from 0.2 to 1 Gy [22]. A direct comparison of our ^{56}Fe ion-induced radiation signature mutations with their AML data show that in both cases increases were observed at the lowest doses tested that decreased at higher doses, a so-called bending of the curve. A similar observation was observed for ^{48}Ti ion-induced radiation signature mutations. A study of Harderian gland tumors induced by a variety of charged particles (^{4}He, ^{12}C, ^{20}Ne, ^{40}Ar, ^{56}Fe) found steep induction curves at low doses (~0.05–0.40 Gy), that leveled off at higher doses, with particle-specific dose-response curves [47]. Weil et al. found similar results for liver cancers induced by ^{56}Fe and ^{28}Si ions [22]. The relevant point of comparison with our mutation data is that radiation-induced tumors were observed at low dose and fluence, which is consistent with our radiation signature mutation data.

5. Conclusions

We showed that whole body exposure to ^{48}Ti and ^{56}Fe ions can induce radiation signature mutations in splenic T cells that are evident at low dose and fluence. Similarly, we observed the induction of radiation signature mutations for a modest dose of protons (0.5 Gy). These consistent observations with three charged particles increase confidence in our findings. Somewhat surprisingly, the induced mutations occurred in the absence of increased mutant frequencies. We hypothesize that this lack of increase reflects either a slower growth rate for a subset of mutant T cells or a more rapid clearance rate of mutant T-cells that may harbor more complex damage. Future work examining mutant frequencies as a function of time after exposure would be required to document this model. Regardless, the presence of radiation signature mutations in the *Aprt* mutant cells isolated from spleens exposed to relatively low doses of high LET ions, and the correlation of our work with tumor models, presents further indication of a cancer risk from prolonged space travel.

Conflict of interest

The authors declare that there are no conflicts of interest.

Acknowledgements

The authors thank Adam Rusek, Peter Guida, Paul Wilson, Mary Ann Petry and their colleagues for support provided for the experiments at Brookhaven National Laboratory. This work was supported by NASA grants NNX10AC12G and NNX14AC97G.

References

[1] J.C. Chancellor, G.B. Scott, J.P. Sutton, Space radiation: the number one risk to astronaut health beyond low earth orbit, Life (Basel) 4 (2014) 491–510.
[2] F.A. Cucinotta, M. Durante, Cancer risk from exposure to galactic cosmic rays: implications for space exploration by human beings, Lancet Oncol. 7 (2006) 431–435.
[3] M. Durante, F.A. Cucinotta, Heavy ion carcinogenesis and human space exploration, Nat. Rev. Cancer 8 (2008) 465–472.
[4] A. Kronenberg, F.A. Cucinotta, Space radiation protection issues, Health Phys. 103 (2012) 556–567.
[5] F.A. Cucinotta, M.H. Kim, L.J. Chappell, J.L. Huff, How safe is safe enough? Radiation risk for a human mission to Mars, PLoS One 8 (2013) e74988.
[6] G. Hryciw, D. Grygoryev, M. Lasarev, A. Ohlrich, C. Dan, R. Madhira, B. Eckelmann, S. Gauny, A. Kronenberg, M.S. Turker, Accelerated (48)Ti ions induce autosomal mutations in mouse kidney epithelium at low dose and fluence, Radiat. Res. 184 (2015) 367–377.
[7] J.F. Davidson, H.H. Guo, L.A. Loeb, Endogenous mutagenesis and cancer, Mutat. Res. 509 (2002) 17–21.
[8] L.A. Loeb, K.R. Loeb, J.P. Anderson, Multiple mutations and cancer, Proc. Natl. Acad. Sci. U. S. A. 100 (2003) 776–781.
[9] P.Y. Chang, N. Kanazawa, L. Lutze-Mann, R. Winegar, HZE particle radiation induces tissue-specific and p53-dependent mutagenesis in transgenic animals, Phys. Med. 17 (Suppl 1) (2001) 189–191.
[10] F. Yatagai, T. Kurobe, T. Nohmi, K. Masumura, T. Tsukada, H. Yamaguchi, K. Kasai-Eguchi, N. Fukunishi, Heavy-ion-induced mutations in the gpt delta transgenic mouse: effect of p53 gene knockout, Environ. Mol. Mutagen. 40 (2002) 216–225.
[11] K. Masumura, K. Kuniya, T. Kurobe, M. Fukuoka, F. Yatagai, T. Nohmi, Heavy-ion-induced mutations in the gpt delta transgenic mouse: comparison of mutation spectra induced by heavy-ion, X-ray, and gamma-ray radiation, Environ. Mol. Mutagen. 40 (2002) 207–215.
[12] R. Lorenz, W. Deubel, K. Leuner, T. Gollner, E. Hochhauser, K. Hempel, Dose and dose-rate dependence of the frequency of HPRT deficient T lymphocytes in the spleen of the 137Cs gamma-irradiated mouse, Int. J. Radiat. Biol. 66 (1994) 319–326.
[13] L. Liang, M.S. Mendonca, L. Deng, S.C. Nguyen, C. Shao, J.A. Tischfield, Reduced apoptosis and increased deletion mutations at Aprt locus in vivo in mice exposed to repeated ionizing radiation, Cancer Res. 67 (2007) 1910–1917.
[14] V.N. Dobrovolsky, J.G. Shaddock, R.H. Heflich, Mutagenecity of gamma-radiation, mitomycin C and etoposide in the Hprt and Tk genes of Tk+/− mice, Environ. Mol. Mutagen. 39 (2002) 342–347.
[15] J.D. Tucker, K.J. Sorensen, C.S. Chu, D.O. Nelson, M.J. Ramsey, C. Urlando, J.A. Heddle, The accumulation of chromosome aberrations and Dlb-1 mutations in mice with highly fractionated exposure to gamma radiation, Mutat. Res. 400 (1998) 321–335.
[16] D.J. Winton, J.H. Peacock, B.A. Ponder, Effect of gamma radiation at high- and low-dose rate on a novel in vivo mutation assay in mouse intestine, Mutagenesis 4 (1989) 404–406.
[17] M.S. Turker, Autosomal mutation in somatic cells of the mouse, Mutagenesis 18 (2003) 1–6.
[18] O.N. Ponomareva, J.A. Rose, M. Lasarev, J. Rasey, M.S. Turker, Tissue-specific deletion and discontinuous loss of heterozygosity are signatures for the mutagenic effects of ionizing radiation in solid tissues, Cancer Res. 62 (2002) 1518–1523.
[19] M.S. Turker, L. Connolly, C. Dan, M. Lasarev, S. Gauny, E. Kwoh, A. Kronenberg, Comparison of autosomal mutations in mouse kidney epithelial cells exposed to iron ions in situ or in culture, Radiat. Res. 172 (2009) 558–566.
[20] A. Kronenberg, S. Gauny, E. Kwoh, G. Grossi, C. Dan, D. Grygoryev, M. Lasarev, M.S. Turker, Comparative analysis of cell killing and autosomal mutation in mouse kidney epithelium exposed to 1 GeV protons in vitro or in vivo, Radiat. Res. 179 (2013) 511–520.
[21] M.H. Barcellos-Hoff, E.A. Blakely, S. Burma, A.J. Fornace Jr., S. Gerson, L. Hlatky, D.G. Kirsch, U. Luderer, J. Shay, Y. Wang, M.M. Weil, Concepts and challenges in cancer risk prediction for the space radiation environment, Life Sci. Space Res. (Amst.) 6 (2015) 92–103.
[22] M.M. Weil, F.A. Ray, P.C. Genik, Y. Yu, M. McCarthy, C.M. Fallgren, R.L. Ullrich, Effects of 28Si ions 56Fe ions, and protons on the induction of murine acute myeloid leukemia and hepatocellular carcinoma, PLoS One 9 (2014) e104819.
[23] P.Y. Chang, R. Doppalapudi, J. Bakke, A. Puey, S. Lin, Evaluation of the impact of shielding materials in radiation protection in transgenic animals, Radiat. Environ. Biophys. 46 (2007) 113–118.
[24] F. Yatagai, T. Nohmi, M. Kusakabe, K. Masumura, A. Yoshiki, H. Yamaguchi, T. Kurobe, K. Kuniya, F. Hanaoka, Y. Yano, Mutation induction by heavy ion irradiation of gpt delta transgenic mice, Biol. Sci. Space 14 (2000) 172–173.
[25] S.B. Curtis, L.W. Townsend, J.W. Wilson, P. Powers-Risius, E.L. Alpen, R.J. Fry, Fluence-related risk coefficients using the Harderian gland data as an example, Adv. Space Res. 12 (1992) 407–416.
[26] E.L. Alpen, P. Powers-Risius, S.B. Curtis, R. DeGuzman, R.J. Fry, Fluence-based relative biological effectiveness for charged particle carcinogenesis in mouse Harderian gland, Adv. Space Res. 14 (1994) 573–581.
[27] T.R. Skopek, V.E. Walker, J.E. Cochrane, T.R. Craft, N.F. Cariello, Mutational spectrum at the Hprt locus in splenic T cells of B6C3F1 mice exposed to *N*-ethyl-*N*-nitrosourea, Proc. Natl. Acad. Sci. U. S. A. 89 (1992) 7866–7870.
[28] Q. Meng, T.R. Skopek, D.M. Walker, S. Hurley-Leslie, T. Chen, D.M. Zimmer, V.E. Walker, Culture and propagation of Hprt mutant T-lymphocytes isolated from mouse spleen, Environ. Mol. Mutagen. 32 (1998) 236–243.
[29] E.E. Furth, W.G. Thilly, B.W. Penman, H.L. Liber, W.M. Rand, Quantitative assay for mutation in diploid human lymphoblasts using microtiter plates, Anal. Biochem. 110 (1981) 1–8.
[30] M.S. Turker, M. Pieretti, S. Kumar, Molecular evidence for the induction of large interstitial deletions on mouse chromosome 8 by ionizing radiation, Mutat. Res. 374 (1997) 201–208.

[31] M.S. Turker, M. Lasarev, L. Connolly, E. Kasameyer, D. Roessler, Age-related accumulation of autosomal mutations in solid tissues of the mouse is gender and cell type specific, Aging Cell 6 (2007) 73–86.
[32] M. Aitkin, D. Anderson, B. Francis, J. Hinde, Statistical Modelling in GLIM, Oxford University Press, New York, 1989.
[33] M. Parzen, S. Lipsitz, J. Ibrahim, J. Klar, An estimate of the odds ratio that always exists, J. Comput. Grap. Stat. 11 (2002) 420–436.
[34] M.S. Turker, B.M. Gage, J.A. Rose, D. Elroy, O.N. Ponomareva, P.J. Stambrook, J.A. Tischfield, A novel signature mutation for oxidative damage resembles a mutational pattern found commonly in human cancers, Cancer Res. 59 (1999) 1837–1839.
[35] J.A. Rose, P.A. Yates, J. Simpson, J.A. Tischfield, P.J. Stambrook, M.S. Turker, Biallelic methylation and silencing of mouse Aprt in normal kidney cells, Cancer Res. 60 (2000) 3404–3408.
[36] M.S. Turker, D. Grygoryev, C. Dan, B. Eckelmann, M. Lasarev, S. Gauny, E. Kwoh, A. Kronenberg, Autosomal mutations in mouse kidney epithelial cells exposed to high-energy protons in vivo or in culture, Radiat. Res. 179 (2013) 521–529.
[37] C. Shao, P.J. Stambrook, J.A. Tischfield, Mitotic recombination is suppressed by chromosomal divergence in hybrids of distantly related mouse strains, Nat. Genet. 28 (2001) 169–172.
[38] A. Kronenberg, Mutation induction in human lymphoid cells by energetic heavy ions, Adv. Space Res. 14 (1994) 339–346.
[39] A. Kronenberg, S. Gauny, E. Kwoh, L. Connolly, C. Dan, M. Lasarev, M.S. Turker, Comparative analysis of cell killing and autosomal mutation in mouse kidney epithelium exposed to 1 GeV/nucleon iron ions in vitro or in situ, Radiat. Res. 172 (2009) 550–557.
[40] M.S. Turker, K.A. Walker, G.D. Jennings, I. Mellon, A. Yusufji, M. Urano, Spontaneous and ionizing radiation induced mutations involve large events when selecting for loss of an autosomal locus, Mutat. Res. 329 (1995) 97–105.
[41] H.L. Liber, R. Idate, C. Warner, S.M. Bailey, Radiation quality and mutagenesis in human lymphoblastoid cells, Radiat. Res. 182 (2014) 390–395.
[42] H.H. Evans, M.F. Horng, T.E. Evans, R. Jordan, J.L. Schwartz, Genotoxic effects of high-energy iron particles in human lymphoblasts differing in radiation sensitivity, Radiat. Res. 156 (2001) 186–194.
[43] N. Okudaira, Y. Uehara, K. Fujikawa, N. Kagawa, A. Ootsuyama, T. Norimura, K. Saeki, T. Nohmi, K. Masumura, T. Matsumoto, Y. Oghiso, K. Tanaka, K. Ichinohe, S. Nakamura, S. Tanaka, T. Ono, Radiation dose-rate effect on mutation induction in spleen and liver of gpt delta mice, Radiat. Res. 173 (2010) 138–147.
[44] P.W. Chang, Q.M. Zhang, K. Takatori, A. Tachibana, S. Yonei, Increased sensitivity to sparsely ionizing radiation due to excessive base excision in clustered DNA damage sites in *Escherichia coli*, Int. J. Radiat. Biol. 81 (2005) 115–123.
[45] P.Y. Chang, J. Bakke, J. Orduna, S. Lin, R. Doppalaudi, Proton-induced genetic damage in lacZ transgenic mice, Radiat. Res. 164 (2005) 481–486.
[46] I.M. Jones, K. Burkhart-Schultz, C.L. Strout, D.O. Nelson, Studies of thioguanine-resistant lymphocytes induced by in vivo irradiation of mice, Environ. Mol. Mutagen. 49 (2008) 343–350.
[47] R.J. Fry, P. Powers-Risius, E.L. Alpen, E.J. Ainsworth, High-LET radiation carcinogenesis, Radiat. Res. (Suppl. 8) (1985) S188–S195.